ACS Sustainable Chemistry & Engineering

Research Article

pubs.acs.org/journal/ascecg

Synthesis of NOM-Capped Silver Nanoparticles: Size, Morphology, Stability, and NOM Binding Characteristics

Susan A. Cumberland[†,§] and Jamie R. Lead*[,†,‡]

[†]School of Geography, Earth and Environmental Sciences, University of Birmingham, Edgbaston, Birmingham B15 2TT, United Kingdom

[‡]Center for Environmental Nanoscience and Risk, Arnold School of Public Health, University of South Carolina, Columbia, South Carolina 29208, United States

Supporting Information

ABSTRACT: Silver nanoparticle synthesis produced by green chemistry methods shows potential in areas such as medical applications and biosensing. Here, we show that natural organic macromolecules (NOM) can be used to synthesize and stabilize silver nanoparticles (AgNPs). Silver nitrate was mixed with one of four NOM types that formed NPs by chemical reduction with either ascorbic acid or sodium borohydride. Resulting NP suspensions were characterized by size, morphology, and stability. A range of particle sizes were obtained, but no clear trends were observed for chemical type or NOM concentration. One reaction (10 mg L^{-1} HA, Ag^{+}, and Na BH_4) produced monodisperse and stable (after three months storage) AgNPs of 10−20 nm, while others such as succinoglycan could be relevant to application in other fields, e.g., medical research. This method indicates the potential to produce relatively stable AgNPs coated with a number of ligands from sustainable sources that are nontoxic and biocompatible, suitable for environmental risk study.

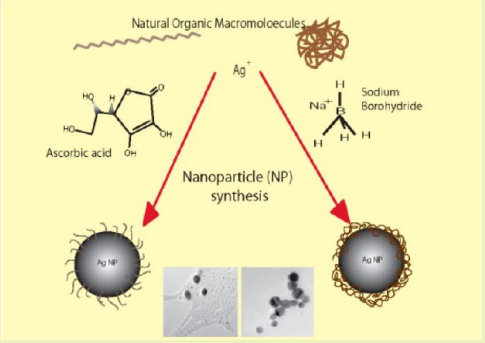

KEYWORDS: *Silver nanoparticles, Natural organic macromolecules, Synthesis, Nanotoxicology, Succinoglycan, Humics*

INTRODUCTION

Manufactured nanoparticles (NPs) (1−100 nm) exhibit different properties from their larger counter parts such as increased specific surface area (SSA), along with altered optical, catalytic, and surface characteristics.[1,2] Commercial exploitation has meant that NPs can now be found in many domestic items including toothpaste, laundry products, food, and food storage materials.[3] Silver nanoparticles (AgNPs) in particular, have received much attention recently due to their antimicrobial properties and wide environmental exposure.[4−6] The presence of NPs in the environment and their high toxicity in many cases[7−12] raises concerns for human and environmental health.

Nanoparticle-capping agents, which are usually organic, are essential to enhance colloidal stability.[13] Metal and metal oxide NPs are typically capped with synthetic chemicals such as citrate, polyethylene glycol (PEG), poly(acrylic acid) (PAA), polyvinylpyrrolidone (PVP), and polyvinyl alcohol (PVA)[14−18] to minimize aggregation. The surface characteristics of NPs are also important in mitigating any toxicity, and capping agents have been found to have a key role here in these processes.[19] Sterically stabilized NPs, in particular, may be expected to be dispersed under all conditions and are therefore potentially more bioavailable and more toxic under realistic environmental conditions.[5,20] In addition, attaching capping agents to NPs, such as quantum dots that reduce solubility and Cd release and thus reduce toxicity,[21] suggests that applying capping agents that are also strong chelators may be ideal in minimizing ion toxicity even after (partial) dissolution of the NPs has occurred.

It is known that presynthesized NPs coated with natural organic macromolecules (NOM), such as humic substances (HS), reduce short-term toxicity of NPs over a range of NP types.[5,22] Therefore, NP formation with NOM is an attractive "green" solution to NP synthesis. However, despite the availability of some published synthesis methods,[23−26] there is a lack of methods that focus on biocompatible chemicals.

A few studies have produced NPs using fresh plant, bacterial, or fungal material[27] resulting in antibacterial wound dressings and fabrics containing NPs.[28,29] Silver NPs have also been manufactured from lemon extract containing 2% citric acid and 0.5% ascorbic acid[30] and inside alfalfa sprouts.[31] It is therefore reasonable to expect that other natural materials would be suitable in NP synthesis, provide NP stability, and perhaps perform better than synthetic chemicals. A number of studies have explored the combination of NPs and natural reagents without other synthetic stabilizers, such as gold capped with humic or fulvic acids for biosensors[24,32,33] and other dried organic materials, such as the *Cinnamomum camphora* leaf, which have been used to produce silver and gold NPs of 65−80 nm.[34]

The work in this paper, which builds on previous work with citrate-Ag NPs and NOM,[35] presents the novel synthesis of

Special Issue: Sustainable Nanotechnology

Received: March 5, 2013
Revised: May 24, 2013
Published: June 20, 2013

1−100 nm silver NPs from four different natural organic macromolecules (NOM) types and two reducing agents, ascorbic acid (AA) and sodium borohydride, $NaBH_4$, without the aid of synthetic ligands. NPs were characterized initially at 24 h and their stability at three months using a range of techniques including visual observation, UV−vis absorbance spectra, transmission electron microscopy (TEM), dynamic light scattering (DLS), and electrophoretic mobility (EPM). This paper highlights the fact that NPs can be formed and stabilized without additional synthetic ligands, which have two implications: (1) NPs can be chemically formed and stabilized in the environment. (2) Such coatings are biologically compatible providing reduced toxicity and allowing the direct study of core particle hazard.

MATERIALS AND METHODS

Materials and Reagent Preparation. Three humic substances were obtained from the International Humic Substance Society (IHSS, Colorado, U.S.): Suwannee River humic acid (HA), Suwannee River fulvic acid (FA), and IHSS peat humic acid (PHA). An exopolysaccharide (PS), succinoglycan, was obtained from Carbomer Inc., U.S., and used at three different concentrations (1, 10, and 100 mg L^{-1}) for the synthesis of AgNPs. Each condition was synthesized with either $NaBH_4$ or ascorbic acid (AA) as the reducing agent. FA and HA stock suspensions (400 mg L^{-1}) were prepared from powder and dissolved in pure water. They were then shaken by hand for 1 min and left in the dark, at 4 °C, for at least 24 h without any further preparation. The PHA stock (400 mg L^{-1}) was prepared from powder and dissolved in pure water with the addition of a few drops of 1 M NaOH to disperse aggregates. Subsequently, the pH was readjusted to pH 7 using 0.1 M NHO_3 to produce a stable suspension at pH 7 with a final concentration of 400 mg L^{-1}. The stock was rapidly mixed to minimize any local effects due to low pH. The PS stock was prepared by dissolving 50.6 mg of powder in 100 mL of pure water. The suspension was stirred for 24 h and then filtered through 0.2 μm preweighed filter papers (Millipore) to remove aggregates. The overall mass was calculated gravimetrically, with a resulting PS concentration of 336 mg L^{-1}. Stock solutions of silver nitrate, $AgNO_3$, 100 mg L^{-1}; sodium borohydride, $NaBH_4$, 38 mg 100 mL^{-1}; and 10^{-2} M ascorbic acid (AA), 178.7 mg 100 mL^{-1} were freshly prepared from their powders in high purity water (UHP, resistivity >18 Ω cm $^{-1}$) and used immediately.

Synthesis of Ag/NOM NP Suspensions. All synthesis steps were performed in 25 mL glass vials at ambient conditions (~20 °C). The NOM (1, 10, or 100 mg L^{-1}) was mixed with $AgNO_3$ solution, 8 mg L^{-1} in water, to a 20 mL volume. After 24 h, 1 mL of the reducing agent stock ($NaBH_4$ or AA) was added and shaken vigorously for 2−3 min. Suspensions were aged under ambient conditions for approximately 8 h and then stored in the dark at 4 °C. All color changes were noted and photographed. In all, 24 reaction conditions were investigated. Resulting suspensions were characterized by UV−vis absorbance, transmission electron microscopy (TEM), dynamic light scattering (DLS), and electrophoretic mobility (EPM) after 24 h and repeated at three months.

NP Suspension Characterization. TEM grids were prepared onto 400 Cu mesh holey carbon film grids (Agar) with samples diluted 10 fold with UHP water to improve particle coverage on the TEM grid, and then 10 μL was dropped onto the grid and then left to dry fully under ambient conditions. Particles were imaged under a 200 keV field emission (FEI) beam using a Philips Technai F20 TEM fitted with Gatan TV Camera, Oxford ISIS EDX, and Gatan digi PEELS detectors.

The imaging areas on TEM were randomly selected and then processed using Gatan DM software, and particle size was derived from all collected images from one or two TEM grids and plotted as histograms. To minimize subjectivity, all particles in the randomly selected frames were included, unless they were either touching the edge of the frame or where a particle could not be distinguished from its neighbor. In total, 2314 particles were measured with an average of about 100 particles for each suspension (Table 1). Standard deviations from TEM are reported from the mean of all particles counted (e.g., ~100 particles per sample).

Hydrodynamic diameter (H_d) (nm) of the suspension was determined by dynamic light scattering (DLS) (Nanosizer, Malvern Instruments) and reported as z-averages and polydispersity index (PDI) of the samples. DLS measurement errors were reported as standard deviations of at least three measurements. Electrophoretic mobility (EPM) (Nanosizer, Malvern Instruments) of the suspensions was also determined. Surface plasmon resonance (SPR) was examined using UV−vis (WMA, Lightwave) light absorbance spectra 200−800 nm.

Statistical Analysis. Statistical information on particle size obtained from TEM images was obtained for comparison by reducing agent, NOM type, and NOM concentration. Histograms were created using Microsoft Excel, and descriptive statistics (standard error (SE), median, mode, st. dev., variance, range distribution, and confidence interval) for TEM particle size were derived from Sigma Plot (Systat Inc.) software. DLS z-average particle size data, used to highlight suspension change and stability on data recorded at 24 h and 3 months, were analyzed using t-tests ($p = 0.05$) or a Mann−Whitney test where data were not normally distributed (Sigma Plot, Systat Inc.).

RESULTS

Suspension Color. Most samples displayed a change in suspension color after adding the reducing agent, which indicated that a reaction had taken place, with possible NP formation. The time taken for the color change to stabilize varied between samples. In particular, there was a notable difference between reducing agents, where silver ion reduction by AA took longer (1−2 h) than $NaBH_4$ (1−2 min). AA reduction produced a greater number of suspensions with an opaque appearance. Yellow suspensions were consistent with silver NPs produced elsewhere using synthetic methods.[35,36] Other colors produced, as indicated by Figure 1, ranged from colorless to yellow, black, brown, and blue, where a blue color is suggestive of the formation of nonsymmetrical NPs[37] and a brown color is suggestive of NP−HS interactions or other HS behavior. The observed blue suspension, shown in Figure 1e, resulted from the $NaBH_4$ reduction with PHA at a concentration of 10 mg L^{-1}, and from TEM, some other shapes were observed, for example, blue suspensions have been linked by Mock et al.[38] to the presence of triangles. Observable color change was not seen in the suspensions produced for the polysaccharide (PS) in the majority of cases, with the exception of the more concentrated 100 mg L^{-1} PS that turned yellow. Color intensity generally increased with high NOM concentrations with the exception of the HA and ascorbic acid reactions. Although the humics may influence the suspension color, final suspensions always resulted in darker coloration than the initial reagents. Higher spectral absorbency readings at $\lambda \sim 254$ nm were recorded with higher NOM concentrations as expected for HS.[35] In contrast, the colorless PS suspensions showed negligible absorbance at $\lambda \sim 254$ nm.

Surface Plasmon Resonance (SPR). The UV−vis absorbance spectra (λ 200−800 nm) of the Ag/NOM suspensions showed broad nonsymmetric peaks in general (Figure S1, Supporting Information), unlike the sharp clean peaks often seen with citrate produced AgNPs, where broad spectrum peaks were likely due to sample (poly)dispersity and absorbance interference from NOM and changes in the refractive index. Those suspensions that resulted in yellow or light brown (e.g., all Ag/HA; Ag/FA 1 and 10 mg L^{-1}; Ag/PHA 1 mg L^{-1}, and Ag/PS 100 mg L^{-1}) gave peaks around λ_{max} 400 nm indicative of Ag NP formation[35] (Figure S1, Supporting Information). The blue suspension (Ag/PHA 10 mg L^{-1}) showed absorbance peaks at longer wavelengths, around 600−700 nm, indicative of shape and other factors such as refractive

Table 1. Silver Nanoparticle Synthesis Conditions and Characterization at 24 h and Three Months[a]

reagent type	NOM type	NOM conc. (mg/L)	absorbance peak max λ_{max} (nm)	TEM (T = 24 h) (nm)	st. dev. (nm)	particles counted (number)	z-average (T = 24 h) (nm)	st. dev. (nm)	PDI	z-average (T = 3 mths) (nm)	st. dev. (nm)	PDI	change in z-average (p < 0.05)	EPM (T = 3 mths) (10^{-8} m^2 V^{-1} s^{-1})	st. dev. (nm)
Na BH_4	HA	1	378	27.8	12.6	101	285.0	13.4	0.4	106.2	1.6	0.4	yes; p = 0.002	−3.11	0.14
		10	384	9.7	3.4	105	19.6	0.8	0.6	20	0.6	0.9	no; p = 0.533	−3.13	0.11
		100	398	8.3	8.8	108	246.9	22.0	0.4	70.2	22.5	1.0	yes; p = 0.024[b]	−2.04	0.41
	FA	1	378	15.3	10.3	163	63.8	2.1	0.6	25.1	0.1	0.6	yes; p < 0.001	−2.56	0.03
		10	398	22.5	13.4	90	13.6	0.4	0.4	17.8	0.5	0.4	yes; p < 0.001	−1.08	0.03
		100	408	11.5	6.9	109	309.3	98.9	0.5	31.4	14.8	0.7	no; p = 0.1[b]	−0.12	0.09
	PHA	1	398	13.3	9.1	70	39.7	14.5	0.3	33	2	0.5	no; p = 0.473	−1.93	0.80
		10	594	19.9	5.2	150	18.0	0.2	0.6	25.1	0	0.7	yes; p < 0.001	−3.26	0.25
		100	321	12.1	5.1	145	159.8	21.7	0.6	128.6	10.9	0.6	no; p = 0.0131	−0.76	0.32
	PS	1	380	5.6	4.7	120	2129.0	167.8	1.0	702.2	3.9	0.5	yes; p < 0.001	−1.35	0.30
		10	392	18.4	19.5	108	428.9	19.8	0.5	387.8	63.4	0.8	no; p = 0.168	−1.27	0.27
		100	394	17.9	14.9	191	200.7	26.3	0.5	173.6	2.4	0.8	no; p = 0.211	−4.78	0.14
AA	HA	1	412	121.7	28.6	83	102.7	1.1	0.1	98.5	1.4	0.1	yes; p = 0.015	−2.99	0.04
		10	538	23.6	27.3	112	177.5	1.9	0.1	162.8	1.2	0.1	yes; p < 0.001	−3.08	0.16
		100	500	52.6	29.8	60	83.8	0.7	0.2	79.2	0.3	0.2	yes; p < 0.001	−2.56	0.08
	FA	1	381	10.6	6.8	179	500.7	22.7	0.2	286.7	90.7	0.3	yes; p = 0.017	−1.81	0.21
		10	376	10.1	7.9	90	276.4	4.5	0.2	150.5	5.2	0.2	yes; p < 0.001	−2.32	0.12
		100	393	31.2	72	67	169.6	3.1	0.2	130.2	0.5	0.1	no; p = 0.1[b]	−3.56	0.02
	PHA	1	382	5.8	2.2	60	–	–	–	136.9	0.9	0.2	n/a	−2.64	0.07
		10	434	66.3	79.9	23	–	–	–	43.5	1.2	0.4	n/a	−2.52	0.11
		100	321	77.4	99.8	21	–	–	–	52	0.5	0.3	n/a	−2.86	0.06
	PS	1	377	–	–	–	–	–	–	353.8	100.6	0.4	n/a	−0.33	0.26
		10	382	5.8	2.4	50	–	–	–	211.6	23.6	0.4	n/a	−1.49	0.18
		100	378	12.1	2.8	109	–	–	–	104	2.9	0.4	n/a	−1.91	0.13
Summary	$NaBH_4$			15.2	12.1	96.6	327.1	572.6		140	193				
	AA			30.3	47.3	318.7	218.5	144.9		150	95				
	1			24.8	36.3	186.2	521.9	773.1		218	221				
	10			16.5	21.1	205.4	155.7	161.5		117	108				
	100			19.2	32.1	318.7	195.0	81.5		96	47				
	PS			13.3	13.4	96.6	923.1	923.6		322	206				
	PHA			19.6	32.6	302.9	72.4	67.4		70	47				
	HA			33.78	42.66	186.10	152.7	96.3		90	46				
	FA			13.6	10.0	93.9	222.2	171.4		107	104				

[a]From transmission electronic microscopy (TEM); z-average (nm) from dynamic light scattering (DLS); polydispersity index (PDI) obtained from DLS measurements; and UV−vis max wavelength (nm) and their corresponding absorbance maximum peaks values. DLS measurements are at 24 h and at three months post synthesis; standard deviations are from three measurements t-test (sigma plot, Systat) applied and Mann−Whitney test applied where marked. Electrophoretic mobility data is at three months only. For all data: mean = 272 nm; SE = 40; median = 146 nm; mode = 272 nm; st. dev. = 452; variance = 203,138; kurtosis = 12; skewness = 3; range = 2346; n = 126 (Excel. [b]Mann−Whitney test performed).

dx.doi.org/10.1021/sc400063r | ACS Sustainable Chem. Eng. 2013, 1, 817−825

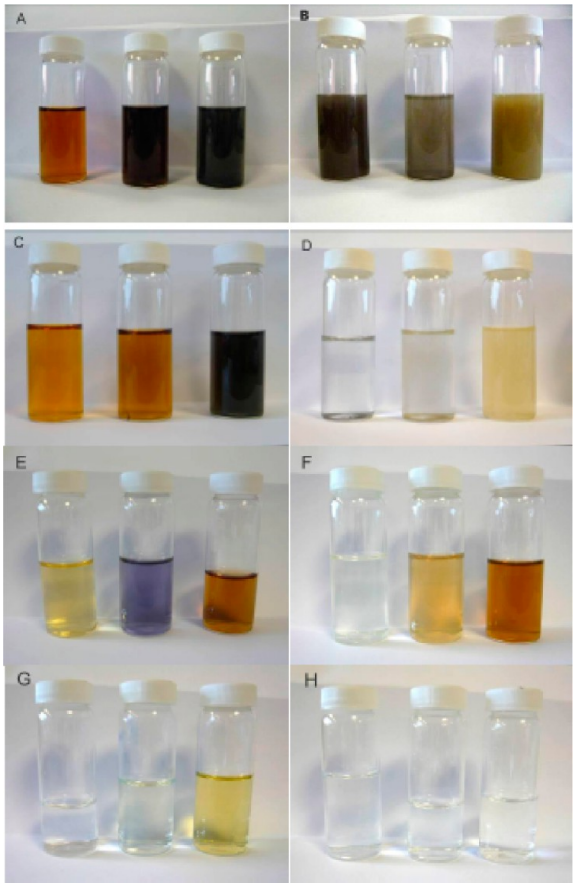

Figure 1. Silver NPs synthesized with NOM 1,10, and 100 mg L^{-1} (left to right): (A) HA and $NaBH_4$, (B) HA with ascorbic acid, (c) FA with $NaBH_4$, (d) FA with ascorbic acid, (E) PHA with $NaBH_4$, (F) PHA with ascorbic acid, (G) PS with $NaBH_4$, and (H) PS with ascorbic acid. Photographs imaged with a digital Panasonic Lumix FX 33 camera.

index, symmetry, and interference of the dipole oscillation.[37−39] The colorless PS suspensions did not reveal any SPR absorbance peaks.

Particle Size. Analysis was performed at 24 h by dynamic light scattering (DLS, z-average) in triplicate, TEM (particle core size), and a polydispersity index (PDI) from DLS (Table 1). Each is reviewed below. According to the DLS z-average, when particle size was examined by NOM type, PHA (72 nm (mean) ± 67 nm (st. dev.)) gave the smallest particle size with PS giving the largest z-average (923 ± 206 nm) providing a size order of PHA < HA = FA < PS (unpaired 2-tailed *t*-test $p < 0.05$). When this data was examined in terms of NOM concentration, the largest particle size was from using 1 mg L^{-1} (522 ± 773 nm), then 10 mg L^{-1} (156 ± 1615 nm), and then 100 mg L^{-1} (195 ± 81 nm), so smallest to largest is 10 < 100 < 1 mg L^{-1} (unpaired 2-tailed *t*-test, $p < 0.05$) When reducing agent conditions were compared, AA z-average was 218 nm compared to $NaBH_4$ with 327 nm (unpaired one-tailed *t*-test $p < 0.05$).

TEM size analysis showed that for NOM concentration, 10 mg L^{-1} overall gave the lowest core particle size (16.5 ± 21.1 nm), followed by 100 mg L^{-1} (19 ± 32 nm), and then 1 mg L^{-1} (25 ± 36 nm); therefore, smallest to largest is 10 < 100 < 1 mg L^{-1} (2-tailed *t*-tests, 1 vs 10 and 1 vs 100, $p < 0.05$, 10 vs 100, $p = 0.052$). Sample variance (distance from the mean, var.) also followed this trend with the 10 mg L^{-1} (var. = 443) displaying lowest variance, and 1 mg L^{-1} (var. = 1320) showing that the 10 mg L^{-1} had less polydispersity than the 1 mg L^{-1} NOM concentration. Standard deviations were higher than the means in all cases. Particle size ranges were similar for 1 and 10 mg L^{-1} (range = 186 and 205 nm) with 100 mg L^{-1} (range = 318 nm) having largest size range and a kurtosis of 44 nm indicating an even particle size distribution (polydisperse). Increasing the concentration of capping agent has been seen to decrease particles size and improve monodispersity.[40,41] However, further increases in capping agent may increase particle size[41] by production of large aggregates from the coalescence of destabilized particles.[42]

For NOM type by TEM, smaller sizes were achieved with PS (13.3 ± 13.4 nm) and FA (13.6 ± 10 nm), but HA (34 ± 43 nm) gave the largest particle size. Particle size for HA was normally distributed (e.g., kurtosis = 1.6, skewness = 1.7), whereas other NOM types showed non-normal distributions indicated by higher kurtosis (>12). Size range was smaller for FA (range = 94 nm, var. = 100 nm) and PS (range = 97 nm, var. = 180 nm) and greater for PHA (range = 303 nm, var. = 1060 nm).

TEM particle size when compared by reducing agent type (AA vs $NaBH_4$, *t*-test $p < 0.05$) was generally smaller for $NaBH_4$ (15.2 ± 12.1 nm) than AA (30 ± 47.3 nm) suspensions, where AA also displayed greater variability in particle size range (range = 318, var. = 2241 nm) compared to $NaBH_4$ (range = 97, var. = 145 nm). However, median and mode values were smaller than the AA mean (median = 10.5 nm, mode = 10.4 nm) indicating longer tailing but similar to $NaBH_4$ mean values (median = 12.2, mode = 13.3). Distribution was near normal for the two data sets. Kurtosis was 9.4 for $NaBH_4$ and 8 for AA indicating some peak broadness and slight one-sided tailing, and skewness was 2.5 for $NaBH_4$ and 2.6 for AA.

Comparison of the z-average and TEM core means of the reactions conditions correlated reasonably well, $r^2 = 0.563$ (TEM = *y*; DLS = *x*; $y = 0.021x + 14.17$) (Figure S3, Supporting Information), where DLS z-averages were larger than TEM core values.

Electrophoretic Mobility (EPM) and Zeta (ζ) Potential. EPM values were negative for all suspensions ranging from -0.12 to -4.78×10^{-8} m^2 V^{-1} s^{-1} ($\zeta = -1.74$ to -67.38 mV) (Figure 6), with suspension Ag/PS 100 mg L^{-1} reduced with $NaBH_4$ being most negative, and FA 100 mg L^{-1} reduced with $NaBH_4$ least negative. In general, better stability is achieved from suspensions that give EPM values greater than $\pm 2.5 \times 10^{-8}$ m^2 V^{-1} s^{-1} ($\zeta > \pm 30$ mV) due to increased particle−particle repulsion. A number of samples in this work had EPM values greater than -2.5×10^{-8} m^2 V^{-1}, indicating stability; however, samples with lower negative charge may also be able to achieve stability through steric stabilization.

Morphology. TEM micrographs of Ag/PHA, Ag/FA, Ag/PS (Figure 2a−f), Ag/HA with $NaBH_4$ (Figure 3a−c), and Ag/HA with AA (Figure 4a−c) showed the presence of many dispersed particles. In other suspensions (Ag/FA 10 mg L^{-1} and Ag/PHA 10 mg L^{-1} with AA), TEM examination revealed that substantial agglomeration had occurred between the Ag and NOM, and these are not presented here. PHA displayed an apparently looser binding that connected several NPs and was not exclusive to a single NP (e.g., Figure 2b). Differences in ligand attachment were seen when PS was used. TEM revealed 1−2 nm particles suspended in the mesh of the PS (Figure 2e), and these particles were too small to be represented in SPR absorbance spectra. Larger NPs and aggregates were also seen to be covered in a thick film of PS as a layer observed in 2-D at the particle surface (Figure 2f). In addition,

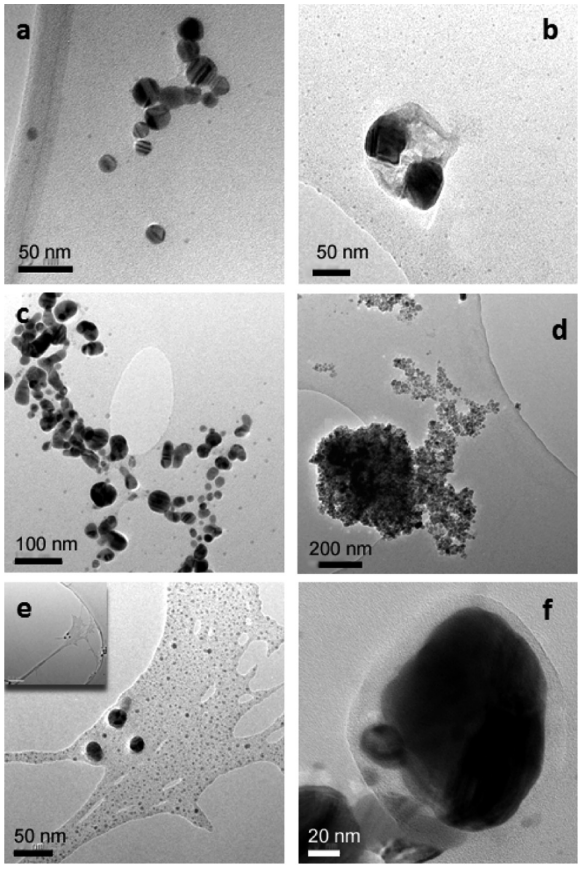

Figure 2. Transmission electron micrographs of silver nanoparticles produced using different NOM capping agents and reduced using either ascorbic acid (AA) or sodium borohydride ($NaBH_4$): (a) peat humic acid 10 mg L^{-1} with $NaBH_4$, (b) peat humic acid 100 mg L^{-1} with AA, (c) Suwannee River fulvic acid 1 mg L^{-1} with $NaBH_4$, (d) Suwannee River fulvic acid 10 mg L^{-1} with $NaBH_4$, (e) polysaccharide 100 mg L^{-1} with $NaBH_4$, and (f) polysaccharide 100 mg L^{-1} with $NaBH_4$ showing thick film attached to silver particle.

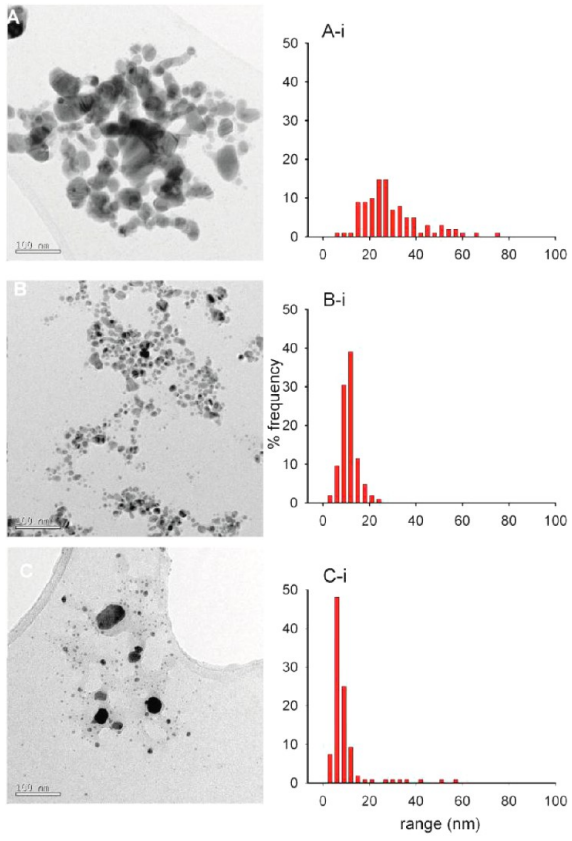

Figure 3. TEM images and particle size representations of TEM (histogram) for silver nanoparticles synthesized with humic acid and a sodium borohydride reduction, where the humic acid concentrations are (a) 1, (b) 10, and (c) 100 mg L^{-1}.

larger spherical agglomerated structures of around ~100 nm were observed (Figure 4a) when using low HA concentrations and AA. NPs produced from PS revealed a small TEM core size but gave very large z-averages; this may be due to the inclusion of the PS molecule in the DLS measurement.

DISCUSSION

Most reactions produced a color change, and yellow suspensions typically result where spherical AgNPs are produced. In this work, from TEM examination, it was evident that nano-sized particles were present in all AgNPs suspensions containing NOM, at all concentrations, and from both reducing agents despite final color. Of the 24 reactions, four suspensions turned yellow; these together gave a mean TEM particle size of 19 nm and a mean z-average of 136 nm, which agrees with size for yellow suspensions from other reported synthesis methods.[18] In addition, many of these reported yellow AgNPs suspensions of around 10−15 nm with spherical NPs also tend to exhibit (SPR) absorbance around λ_{max} 390 nm.[43] Some suspensions produced in this work displayed a non-yellow color but also had particle means of <20 nm (TEM). The observed non-yellow color is likely to result from modifications in SPR due to NOM attachment at the AgNP's surface.[44] However, the relationship between size and color appears to be less clear cut when applied to nonsymmetrical particles[38] or agglomeration and presence of larger particle size.[43,45]

TEM images showed that particles were formed in all reactions containing PS and revealed evidence of very small particles of about 1−2 nm nested within a matrix of PS. A few of the PS suspensions remained colorless even after the reducing agent had been added; these colorless PS suspensions also revealed an absence of well-defined SPR bands. According to the Mie theory, SPR peaks are likely to be absent for particles less than 2 nm or greater than 50 nm[45] due to the discrete electronic states of the molecular clusters in very small particles, and the inability for larger NPs to polarize light.[45] The fact that NPs could be synthesized within an organic polymer gel such as the exopolysaccharide succinoglycan used here opens up interesting future research opportunities.

Variations and peak broadness in SPR absorbance spectra observed with the NPs in this work may be attributed to optical interferences occurring at the NP surface either from the NOM itself, its attachment, or associated functional groups. Ligands attached to NP surfaces have also been found to alter SPR peak sharpness to varying degrees,[43] and interferences from NOM gave rounded and nonsymmetrical SPR spectral peaks analogous as to those observed by Akaighe et al.[23] for HA-capped AgNPs and Dos Santos et al.[33] with FA and Au NPs. This supports the results presented in this paper where peaks in the SPR spectra were either broadly defined or absent, despite the presence of small particles from TEM examination.

Some suspensions also revealed absorbance around λ 250 nm, which was evident in AA suspensions and absent in suspensions

dx.doi.org/10.1021/sc400063r | ACS Sustainable Chem. Eng. 2013, 1, 817−825

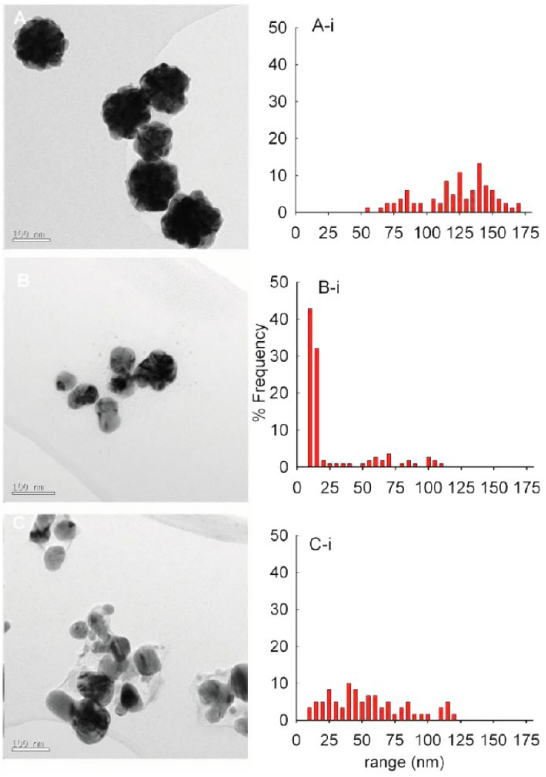

Figure 4. TEM images and particle size representations of TEM (histogram) for silver nanoparticles synthesized with humic acid and an ascorbic acid reduction, where the humic acid concentrations are (a) 1, (b) 10, and (c) 100 mg L^{-1}.

with $NaBH_4$. While this could be attributed to humics alone (Abs λ 254 nm), the peak was also present in PS suspensions. Analysis of a pure AA solution revealed absorbance at λ_{max} 250 nm not present from a similar pure solution of $NaBH_4$[41] suggesting that the peak was from the AA in our samples. Its absence after 3 months implies that the reaction was incomplete at 24 h, and its reduction was probably due to the continual breakdown of the AA product to other chemical species.[46]

Particles reduced with AA were larger, although not significantly, than those AgNPs reduced with $NaBH_4$, with a greater particle size range (compare Figure 3 to Figure 4). Ag NPs made through AA reductions have been reported to have a slower growth process and are often used with capping agents of higher molecular weight.[14,47,48] Reduction of absorbance at λ 250 nm on remeasurement at 3 months supports the slower reaction time, which may in itself promote larger and wider ranges of particle sizes. This indication toward longer reaction times of the AA to reach stability may be evident from its reaction with silver nitrate. Described by Stathis,[46] the reaction, eq 1, demonstrates the final production of nitric acid, which may in turn affect localized pH change at NP surfaces, promoting instability and the potential toward silver dissolution to Ag^+.

$$2AgNO_3 + C_6H_8O_6 \rightarrow 2Ag + C_6H_6O_6 + 2HNO_3 \quad (1)$$

The role that NOM plays in this equation is unknown, but NOM may provide the AgNP surface with protection against HNO_3. It is noteworthy that NP synthesis methods in the literature that employ AA as a reagent also use ligands of high molecular weight.[14,47,48] In comparison, the exact nature of the reaction with borohydride is unclear from the literature as borohydride dissociates in water prior to contact with the silver ion with the slow release of H_2 gas bubbles.[18]

Given the borohydride dissociation, emphasis can be placed on the importance of using only freshly made solutions to reduce Ag^+ ions. Furthermore, the formation of NPs may depend on the rate of addition of the reducing agent to the Ag^+,[41] while others have found the reaction to be affected by pH.[47] Freshly made suspensions also require being left for 24 h for reactions to complete in order to "age".[41]

As postulated by Pal et al.,[49] eq 2 shows that the $NaBH_4$ reaction with silver nitrate results in a production of hydrogen gas and boric acid, a weaker acid ($Ka = 5.8 \times 10^{-10}$) compared to nitric acid ($Ka = 2.4$).

$$2AgNO_3 + 2NaBH_4 + 6H_2O \rightarrow 2Ag + 2NaNO_3 + 2H_3BO_3 + 7H_2 \quad (2)$$

It is unlikely that in the absence of a capping agent, NPs would be able to remain in suspension under the conditions of eq 1 given the nitric acid byproduct and tendency to aggregate. Uncertainties also exist in the effect of nitric acid on the NP surface causing localized lowering of pH. In the reaction involving borohydride, a capping agent is again necessary to prevent the BH_4^- ion sorbing to the silver particles' surface and reoxidizing the Ag.[49]

The most likely mechanism of NOM attachment to Ag^0 NP's surface is through its functional groups. One such group present in humic substances, but not PS, is thiol, which is known have a strong affinity for silver. In our experiments, NOM bonding to silver may have occurred prior to NP formation because the $AgNO_3$ and NOM was premixed (24 h) before the introduction of either reducing agent. Other possible bonding mechanisms are to oxide and hydroxide layers that may be present on the NP's surface, although our other as yet unpublished work suggests that such layers do not readily form in aqueous systems.

NP Suspensions Stability. All suspensions appeared visually to be identical at 3 months compared to when first made with no obvious signs of color loss or formation of sediments after storage at +4 °C in the dark. Figure 5 shows the change in particle size of the Ag/NOM NPs for all conditions at T = 24 h and T = 3 months for SPR and z-average. The $NaBH_4$ AgNPs suspensions showed less reduction in SPR absorbance (Figure 5, compare Figures S1 and Figure S2, Supporting Information) than AA, over time indicating greater stability. DLS measurements at T = 24 h and T = 3 months from Table 1 show that seven suspensions were identified as having no change in particle size ($p < 0.05$) over time that demonstrates suspension stability. Two of these seven suspensions were reasonably monodisperse Ag/HA 10 mg L^{-1} with $NaBH_4$ and Ag/PHA 10 mg L^{-1} with $NaBH_4$. Observed particle size increase indicates that growth, through aggregation, has occurred. Particle size decrease, on the other hand, can signify particle removal through sedimentation.

Cumberland and Lead[35] showed that additions of NOM to citrate AgNPs improved stability at pH 5 and 8 and increased ionic strength in the presence of calcium, compared to citrate only capped AgNPs. It is therefore likely that pure NOM AgNPs will behave similarly. The difference between the particles made here and those covered in citrate and then exposed to NOM later demonstrate that this method enables NOM-facilitated stabilization of AgNPs from a direct exposure of Ag to humics

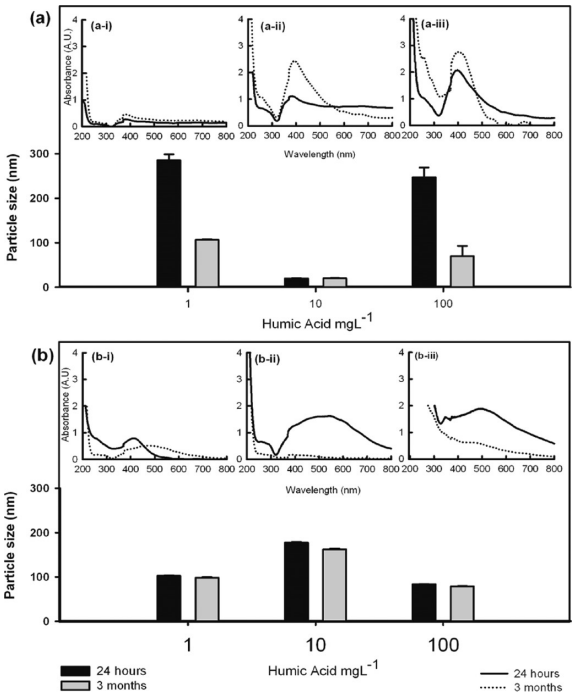

Figure 5. HA/AgNPs (1, 10, and 100 mg L^{-1} HA) made with (a) $NaBH_4$ and (b) ascorbic acid, measured at 24 h and 3 months for suspensions particle size by DLS. Inserts (a, i–iii) and (b, i–iii) are the SPR absorbance graphs recorded at 24 h and 3 months for each HA concentration (1, 10, 100 mg L^{-1}), respectively.

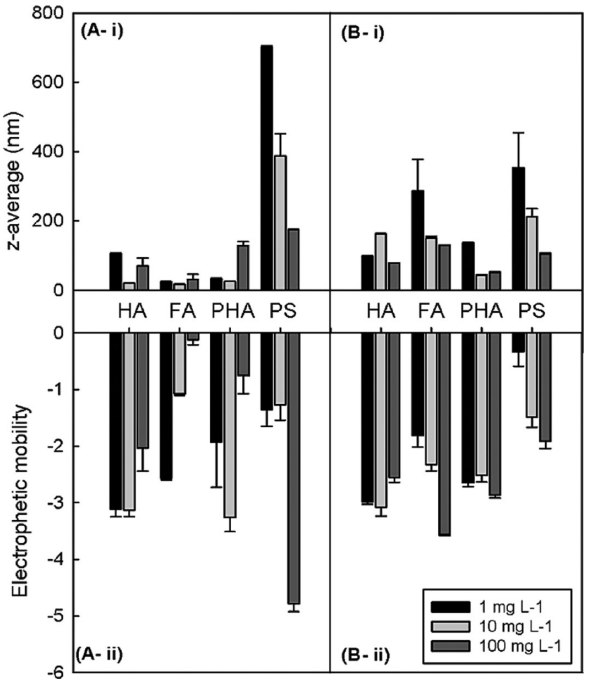

Figure 6. Top (A, i; B, i) DLS z-average(nm) and bottom (A, ii; B, ii) electrophoretic mobility (10^{-8} m^2 V^{-1} s^{-1}) for left (A, i; A, ii) sodium borohydride and right (B, i; B, ii) ascorbic acid. Error bars are standard deviations.

using fewer processing steps, thus eliminating the need to presynthesis NPs prior to adding NOM.

Size Differences between TEM and DLS. Comparisons in particle size between techniques for the same suspensions revealed that DLS z-averages were on average larger, by almost an order of magnitude, than particles size derived from TEM images (Figure S3, Supporting Information). Variations between DLS and TEM particle size are not unusual and are legitimately attributed to the differences in methods employed by each technique. For instance, DLS obtains its particle size derived from diffusion coefficients (converted to H_d via the Stokes–Einstein equation) through backscatter detection from Brownian motion.[50−52,48−50] DLS is also particularly sensitive to small amounts of large particles either from aggregation, bridging, larger Ag particles, or contamination;[53] inclusion of surface bound NOM coatings and could also include measurement of free NOM unbound to AgNPs[53,54] thus increasing the size of the DLS H_d. TEM on the other hand is a direct measurement of the particle's core, which is often visibly absent of any particle coatings, although if humic matter is present it can be partially visible under the electron beam. Good agreement occurs between DLS and TEM for particles when they are monodispersed, monomodal, unaggregated, and without capping agents that are of substantial size.

Electrophoretic Mobility. There was no overall consistency for EPM for a given NOM type for individual measurements (Figure 6). However, there was an inverse correlation between mean TEM and EPM values (r^2 = 0.96) by NOM type, indicating that NOM type was more influential than NOM concentration or reducing agent type, with humic acid having the most negative value (EPM = 2.82×10^{-8} m^2 V^{-1} s^{-1}; ζ = −39 mV). The most stable AgNP was synthesized with 10 ppm HA with $NaBH_4$ and also had a high ζ value. Others have also found a correlation between high ζ and small particle size, which occurs when the particles are statically or charge stabilized, and thus stability is affected by pH and ionic strength. In this case, the NOM is affecting the measurement, and the true slipping value cannot be achieved. The results here indicate that stabilization was achieved by electrosteric stabilization rather than simply electrostatically, although some negative charge from the NOM types used here will also influence stability.

Suitability for Nanotoxicity Study. In order to more fully understand NP toxicity, it is important to understand, among other things, whether toxicity arises from small particle size, dissolution, surface properties, particle aggregation, or reaction with biological test media. Nanoparticles considered suitable for applying to nanoparticle toxicology and eco-toxicological studies are ideally required to fall within certain criteria: narrow particle size range with a number of particle sizes available, nontoxic capping agent, particle stability at neutral pH, and higher ionic strength. NOM has been shown to be good at stabilizing NPs over a range of pH and ionic strengths with synthetically capped silver nanoparticles.[32] Having test materials that comply with the above criteria will help increase the current knowledge to further provide information about the mechanisms and drivers that cause NP toxicity and bioavailability following exposure. The nanoparticles synthesized in this work show potential in this area. The most stable and monodisperse nanoparticle suspension in this study was determined to be Ag HA 10 mg L^{-1} reduced using $NaBH_4$.

■ ASSOCIATED CONTENT

Supporting Information

Figures S1 and S2, which show the UV–vis absorbance SPR plots of the silver nanoparticles suspensions at T = 24 h and T = 3 months. Figure S3 is a correlation plot between means of

DLS- and TEM-derived particle size by experimental condition. This material is available free of charge via the Internet at http://pubs.acs.org.

AUTHOR INFORMATION

Corresponding Author

*E-mail: jlead@mailbox.sc.edu.

Present Addresses

[§]Susan A. Cumberland: School of Earth Sciences, University of Melbourne, Parkville 3031, Melbourne, Victoria, Australia.

Author Contributions

The manuscript was written through contributions of all authors. All authors have given approval to the final version of the manuscript.

Notes

The authors declare no competing financial interest.

ACKNOWLEDGMENTS

This work was funded by a NERC grant NE/D004942/1 and studentship NER/S/J/2005/13991. Thanks also to Ming Chu for help with TEM and Dr. Gillian Kingston for laboratory support.

REFERENCES

(1) Auffan, M.; Rose, J.; Bottero, J.-Y.; Lowry, G. V.; Jolivet, J.-P.; Wiesner, M. R. Towards a definition of inorganic nanoparticles from an environmental, health and safety perspective. *Nature Nanotechnol.* **2009**, *4*, 634.

(2) Nikolakis, V. Understanding the effect of specific surface area and surface reactions on silicalite-1 nucleation and growth. *Microporous Mesoporous Mater.* **2006**, *93*, 101.

(3) Schmid, K.; Riediker, M. Use of nanoparticles in Swiss industry: A targeted survey. *Environ. Sci. Technol.* **2008**, *42*, 2253.

(4) Carlson, C.; Hussain, S. M.; Schrand, A. M.; K. Braydich-Stolle, L.; Hess, K. L.; Jones, R. L.; Schlager, J. J. Unique cellular interaction of silver nanoparticles: Size-dependent generation of reactive oxygen species. *J. Phys. Chem. B* **2008**, *112*, 13608.

(5) Fabrega, J.; Fawcett, S. R.; Renshaw, J. C.; Lead, J. R. Silver nanoparticle impact on bacterial growth: effect of pH, concentration and organic matter. *Environ. Sci. Technol.* **2009**, *43*, 7285.

(6) Nowack, B. The behavior and effects of nanoparticles in the environment. *Environ. Pollut.* **2009**, *157*, 1063.

(7) Alvarez, P. J. J.; Colvin, V.; Lead, J.; Stone, V. Research priorities to advance eco-responsible nanotechnology. *ACS Nano* **2009**, *3*, 1616.

(8) Zhu, X.; Zhu, L.; Chen, Y.; Tian, S. Acute toxicities of six manufactured nanomaterial suspensions to *Daphnia magna*. *J. Nanopart. Res.* **2009**, *11*, 67.

(9) Pettitt, M. E.; Lead, J. R. Minimum physicochemical characterisation requirements for nanomaterial regulation. *Environ. Int.* **2013**, *52*, 41.

(10) Ju-Nam, Y.; Lead, J. R. Manufactured nanoparticles: An overview of their chemistry, interactions and potential environmental implications. *Sci. Total Environ.* **2008**, *400*, 396.

(11) Klaine, S. J.; Alvarez, P. J. J.; Batley, G. E.; Fernandes, T. F.; Handy, R. D.; Lyon, D. Y.; Mahendra, S.; McLaughlin, M. J.; Lead, J. R. Nanomaterials in the enviornment: Behavior, fate, bioavailability, and effects. *Environ. Toxicol. Chem.* **2008**, *27*, 1825.

(12) Fabrega, J.; Renshaw, J. C.; Lead, J. R. Interactions of silver nanoparticles with *Pseudomonas putida* biofilms. *Environ. Sci. Technol.* **2009**, *43*, 9004.

(13) Christian, P.; Von der Kammer, F.; Baalousha, M.; Hofmann, T. Nanoparticles:Structure, properties, preparation and behaviour in environmental media. *Ecotoxicology* **2008**, *17*, 326.

(14) Henglein, A.; Giersig, M. Formation of colloidal silver nanoparticles: Capping action of citrate. *J. Phys. Chem. B* **1999**, *103*, 9533.

(15) Ledwith, D. M.; Whelan, A. M.; Kelly, J. M. A rapid, straightforward method for controlling the morphology of stable silver nanoparticles. *J. Mater. Chem.* **2007**, *17*, 2459.

(16) Pillai, Z. S.; Kamat, P. V. What factors control the size and shape of silver nanoparticles in the citrate ion reduction method? *J. Phys. Chem. B* **2003**, *108*, 945.

(17) Sun, Y.; Xia, Y. Shape-controlled synthesis of gold and silver nanoparticles. *Science* **2002**, *298*, 2176.

(18) Van Hyning, D. L.; Zukoski, C. F. Formation mechanisms and aggregation behavior of borohydride reduced silver particles. *Langmuir* **1998**, *14*, 7034.

(19) Tejamaya, M.; Römer, I.; Merrifield, R. C.; Lead, J. R. Stability of citrate, PVP, and PEG coated silver nanoparticles in ecotoxicology media. *Environ. Sci. Technol.* **2012**, *46*, 7011.

(20) Hitchman, A.; Ju-Nam, Y.; Sambrook-Smith, G.; Sterling, M.; Lead, J. R. The effect of environmentally relevant conditions on PVP stabilised gold nanoparticles. *Chemosphere* **2013**, *90*, 410.

(21) Aruguete, D. M.; Guest, J. S.; Yu, W. W.; Love, N. G.; Hochella, M. F. Interaction of CdSe/CdS core-shell quantum dots and *Pseudomonas aeruginosa*. *Environmental Chemistry* **2010**, *7*, 28.

(22) Li, D.; Lyon, D. Y.; Li, Q.; Alvarez, P. J. J. Effect of soil sorption and aquatic natural organic matter on the antibacterial activity of a fullerene water suspension. *Environ. Toxicol. Chem.* **2008**, *27*, 1888.

(23) Akaighe, N.; MacCuspie, R. I.; Navarro, D. A.; Aga, D. S.; Banerjee, S.; Sohn, M.; Sharma, V. K. Humic acid-induced silver nanoparticle formation under environmentally relevant conditions. *Environ. Sci. Technol.* **2011**, *45*, 3895.

(24) Dubasa, S. T.; Pimpan, V. Humic acid assisted synthesis of silver nanoparticles and its application to herbicide detection. *Mater. Lett.* **2008**, *62*, 2661.

(25) Mohanpuria, P.; Rana, N.; Yadav, S. Biosynthesis of nanoparticles: Technological concepts and future applications. *J. Nanopart. Res.* **2008**, *10*, 507.

(26) Huang, H.; Yang, X. Synthesis of polysaccharide-stabilized gold and silver nanoparticles: A green method. *Carbohydr. Res.* **2004**, *339*, 2627.

(27) Shaligram, N. S.; Bule, M.; Bhambure, R.; Singhal, R. S.; Singh, S. K.; Szakacs, G.; Pandey, A. Biosynthesis of silver nanoparticles using aqueous extract from the compactin producing fungal strain. *Process Biochem.* **2009**, *44*, 939.

(28) Maneerung, T.; Tokura, S.; Rujiravanit, R. Impregnation of silver nanoparticles into bacterial cellulose for antimicrobial wound dressing. *Carbohydr. Polym.* **2008**, *72*, 43.

(29) Duran, N.; Marcato, P. D.; De Souza, G. I. H.; Alves, O. L.; Esposito, E. Antibacterial effect of silver nanoparticles produced by fungal process on textile fabrics and their effluent treatment. *J. Biomed. Nanotechnol.* **2007**, *3*, 203.

(30) Prathna, T. C.; Chandrasekaran, N.; Raichur, A. M.; Mukherjee, A. Biomimetic synthesis of silver nanoparticles by Citrus limon-(lemon) aqueous extract and theoretical prediction of particle size. *Colloids Surf., B* **2011**, *82*, 152.

(31) Gardea-Torresdey, J. L.; Gomez, E.; Peralta-Videa, J. R.; Parsons, J. G.; Troiani, H.; Jose-Yacaman, M. Alfalfa sprouts: A natural source for the synthesis of silver nanoparticles. *Langmuir* **2003**, *19*, 1357.

(32) Alvarez-Puebla, R. A.; dos Santos, D. S., Jr.; Aroca, R. F. SERS detection of environmental pollutants in humic acid−gold nanoparticle composite materials. *Analyst* **2007**, *132*, 1210.

(33) dos Santos, D. S., Jr; Alvarez-Puebla, R. A.; Oliveira, O. N., Jr; Aroca, R. F. Controlling the size and shape of gold nanoparticles in fulvic acid colloidal solutions and their optical characterization using SERS. *J. Mater. Chem.* **2005**, *15*, 3045.

(34) Huang, J.; Li, Q.; Sun, D.; Lu, Y.; Su, Y.; Yang, X.; Wang, H.; Wang, Y.; Shao, W.; He, N.; Hong, J.; Chen, C. Biosynthesis of silver and gold nanoparticles by novel sundried *Cinnamomum camphora* leaf. *Nanotechnology* **2007**, *18*, 105104.

(35) Cumberland, S. A.; Lead, J. R. Particle size distributions of silver nanoparticles at environmentally relevant conditions. *J. Chromatogr., A* **2009**, *1216*, 9099.

(36) Römer, I.; White, T. A.; Baalousha, M.; Chipman, K.; Viant, M. R.; Lead, J. R. Aggregation and dispersion of silver nanoparticles in exposure media for aquatic toxicity tests. *J. Chromatogr., A* **2011**, *1218*, 4226.
(37) Sun, Y.; Xia, Y. Triangular nanoplates of silver: synthesis, characterization, and use as sacrificial templates for generating triangular nanorings of gold. *Adv. Mater.* **2003**, *15*, 695.
(38) Mock, J. J.; Barbic, M.; Smith, D. R.; Schultz, D. A.; Schultz, S. Shape effects in plasmon resonance of individual colloidal silver nanoparticles. *J. Chem. Phys.* **2002**, *116*, 6755.
(39) Lee, K.-S.; El-Sayed, M. A. Gold and silver nanoparticles in sensing and imaging: Sensitivity of plasmon response to size, shape, and metal composition. *J. Phys. Chem. B* **2006**, *110*, 19220.
(40) Rivas, L.; Sanchez-Cortes, S.; Garcia-Ramos, J. V.; Morcillo, G. Growth of silver colloidal particles obtained by citrate reduction to increase the Raman enhancement factor. *Langmuir* **2001**, *17*, 574.
(41) Cumberland, S. A. Synthesis and Environmental Chemistry of Silver and Iron Oxide Nanoparticles. Thesis, University of Birmingham, 2011.
(42) Baalousha, M. Aggregation and disaggregation of iron oxide nanoparticles: Influence of particle concentration, pH and natural organic matter. *Sci. Total Environ.* **2009**, *407*, 2093.
(43) MacCuspie, R. I.; Rogers, K.; Patra, M.; Suo, Z.; Allen, A. J.; Martin, M. N.; Hackley, V. A. Challenges for physical characterization of silver nanoparticles under pristine and environmentally relevant conditions. *J. Environ. Monit.* **2011**, *13*, 1212.
(44) Miller, M. M.; Lazarides, A. A. Sensitivity of metal nanoparticle plasmon resonance band position to the dielectric environment as observed in scattering. *J. Opt. A: Pure Appl. Opt.* **2006**, S239.
(45) Link, S.; El-Sayed, M. A. Optical properties and ultrafast dynamics of metallic nanocrystals. *Annu. Rev. Phys. Chem.* **2003**, *54*, 331.
(46) Stathis, E. C. Determination of silver with ascorbic acid. *Anal. Chem.* **1948**, *20*, 271.
(47) Sondi, I.; Goia, D. V.; Matijevic, E. Preparation of highly concentrated stable dispersions of uniform silver nanoparticles. *J. Colloid Interface Sci.* **2003**, *260*, 75.
(48) Suber, L.; Sondi, I.; Matijevic, E.; Goia, D. V. Preparation and the mechanisms of formation of silver particles of different morphologies in homogeneous solutions. *J. Colloid Interface Sci.* **2005**, *288*, 489.
(49) Pal, T.; Sau, T. K.; Jana, N. R. Reversible formation and dissolution of silver nanoparticles in aqueous surfactant media. *Langmuir* **1997**, *13*, 1481.
(50) Kaszuba, M.; McKnight, D.; Connah, M.; McNeil-Watson, F.; Nobbmann, U. Measuring sub nanometre sizes using dynamic light scattering. *J. Nanopart. Res.* **2008**, *10*, 823.
(51) Diegoli, S.; Manciulea, A. L.; Begum, S.; Jones, I. P.; Lead, J. R.; Preece, J. A. Interaction between manufactured gold nanoparticles and naturally occurring organic macromolecules. *Sci. Total Environ.* **2008**, *402*, 51.
(52) Baalousha, M.; Lead, J. R. Rationalizing nanomaterial sizes measured by atomic force microscopy, flow field-flow fractionation, and dynamic light scattering: sample preparation, polydispersity, and particle structure. *Environ. Sci. Technol.* **2012**, *46*, 6134.
(53) Domingos, R. F.; Baalousha, M. A.; Ju-Nam, Y.; Reid, M.; Tufenkji, N.; Lead, J. R.; Leppard, G. G.; Wilkinson, K. J. Characterizing manufactured nanoparticles in the environment: Multimethod determination of particle sizes. *Environ. Sci. Technol.* **2009**, *43*, 7277.
(54) Baalousha, M.; Lead, J. R. Characterization of natural aquatic colloids (<5 nm) by flow-field flow fractionation and atomic force microscopy. *Environ. Sci. Technol.* **2007**, *41*, 1111.